Visually Exploring Differences of DTI Fiber Models

Honghui Mei[1], Haidong Chen[1], Fangzhou Guo[1], Fan Zhang[2], Wei Chen[1(✉)], Zhang Song[3], and Guizhen Wang[1]

[1] State Key Lab of CAD&CG, Zhejiang University, Hangzhou, China
meihonghui.zju@gmail.com, chenhd925@gmail.com, guofz1234@gmail.com, wguizhen@gmail.com, chenwei@cad.zju.edu.cn
[2] Zhejiang University of Technology, Hangzhou, China
fanzhang@cad.zju.edu.cn
[3] Computer Science and Engineering, Mississippi State University, Starkville, USA
szhang@cse.msstate.edu

Abstract. Fiber tracking of Diffusion Tensor Imaging (DTI) datasets is a non-invasive tool to study the underlying fibrous structures in living tissues. However, DTI fibers may vary from subject to subject due to variations in anatomy, motions in scanning, and signal noise. In addition, fiber tracking parameters have a great influence on tracking results. Subtle changes of parameters can produce significantly different DTI fibers. Interactive exploration and analysis of differences among DTI fiber models are critical for the purposes of group comparison, atlas construction, and uncertainty analysis. Conventional approaches illustrate differences in the 3D space with either voxel-wise or fiber-based comparisons. Unfortunately, these approaches require an accurate alignment process and might give rise to visual clutter. This paper introduces a two-phase projection technique to reformulate a complex 3D fiber model as a unique 2D map for feature characterization and comparative analysis. To facilitate investigation, regions of significant differences among the 2D maps are further identified. Using these maps, differences that are difficult to be distinguished in the 3D space due to depth occlusion can be easily discovered. We design a visual exploration interface to study differences from multiple perspectives. We evaluate the effectiveness of our approach by examining two datasets.

Keywords: Diffusion tensor imaging · Fiber tracking · Difference visualization · Visual exploration

1 Introduction

Diffusion Tensor Imaging (DTI) [2] is a non-invasive *in vivo* magnetic resonance imaging technique that measures the diffusion of water in biological tissues. In tissues containing fibrous structures, the diffusion is faster along the fibers [14]. By fitting the distribution with a Gaussian model, a DTI tensor volume can

A. El Rhalibi et al. (Eds.): Edutainment 2016, LNCS 9654, pp. 333–344, 2016.
DOI: 10.1007/978-3-319-40259-8_29

be reconstructed from the raw Diffusion Weighted Imaging (DWI) volumes [24]. Tracing paths through the entire tensor volume produces a collection of DTI fibers. This process is known as fiber tractography or fiber tracking [1], which has been proven to be a useful technique for analyzing anatomical connectivity.

In spite of its potential, DTI remains limited in applications. Uncertainty is a major reason. DTI fibers vary from subject to subject due to variations in anatomy, and from scan to scan because of different subject positions, scanning motions and noises [14]. They are also sensitive to various parameters in tractography such as the integration step size and stopping criteria [3].

To comparatively visualizing and analyzing different DTI datasets, one of the major task is to represent and visualize differences within a collection of DTI datasets. Direct comparison of 3D DWI or DTI volumes [18,28] demands an accurate alignment process and misses the anatomical connectivity within each volume. Explicit depiction of the geometrical differences among DTI fiber models in the 3D space [3,7] is hindered by the spatial complexity of dense fibers. Comparison by using statistical tractography metrics [6] lacks the ability to locate regions of differences.

Projection techniques have been widely used to provide a holistic view of the overall structures and distributional patterns. Recent work extends this scheme into the exploration of DTI fiber models [4,25]. However, these solutions are well designed to explore the content of only a single fiber model. The main reason is that different fiber models do not share a common space for projection and comparison.

In this paper, we present a comparative visualization approach that supports quick identification and intuitive exploration of differences among DTI fiber models. After all datasets are registered into a common coordinate space, fiber models are embedded on a 2D visual plane by means of a two-phase projection technique. The embedding of a fiber model constructs a 2D scatterplot which are further represented as a continuous density map and a contoured density map. To provide an overview of the major differences among these maps, regions of differences (RoDs) are computed with a simple flood fill algorithm. Both *Juxtaposition* and *Explicit Encoding* are utilized within the visual exploration interface. We have verified the effectiveness of our approach on several DTI datasets.

In summary, the contributions of this paper are:

- A novel low-dimensional representation of complex fiber models for visual comparison and further regions of differences identification;
- An integrated visualization interface that provides users an intuitive way to explore differences in multiple perspectives.

The remaining parts are organized as follows. Related work are summarized in Sect. 2. Our approach is elaborated in Sect. 3. The visual exploration interface is described in Sect. 4. The results of our approach are discussed in Sect. 5. Finally, we conclude this paper in Sect. 6.

2 Related Work

Our work is related to several topics of visualization research including comparative visualization, uncertainty visualization, and DTI fiber model exploration.

2.1 Comparative Visualization

Recently, a wide variety of approaches have been developed in the field of comparative visualization. Gleicher et al. [12] summarized visual designs for comparisons into three categories: *Juxtaposition*, *Superposition*, and *Explicit Encoding*. Verma and Pang [29] proposed several solutions for comparative flow visualization at image level, data level, and feature level. Malik et al. [20] introduced a novel multi-view design for comparing and visualizing gray values and edges of several 3D CT datasets simultaneously. Schmidt et al. [26] proposed an approach for comparative visualization of multiple images. Their technique overcomes the scalability issues pertaining to the number of objects for comparison, and allows users to perform detailed cluster analysis in the regions of significant differences. Oelke et al. [22] designed a glyph representation called topic coins to encode information necessary for comparative document analysis.

In the field of DTI study, comparison is an important means to locate changes related to development, degeneration, and disease. One pioneering work [7] compares the generated fibers in the 3D space and uses saturation to indicate the magnitude of differences between corresponding points. This method is simple and intuitive, but only focuses on fiber structures and may result in visual clutter. In order to investigate the diffusion properties along fibers, group statistical analysis [5,13] is performed after aligning datasets and representing fibers with continuous functions. The key idea behind this method is that fibers are represented with a simplified form (like B-spline) to facilitate statistical comparison.

To study the diffusion property volumes such as the Fractional Anisotropy (FA) for multiple subjects, Smith et al. [28] presented Tract-Based Spatical Statistics (TBSS), which is a voxel wise analysis framework via a nonlinear registration followed by projection onto a skeleton. In addition to the study on DTI volumes, there has been some work on general-purpose group analysis of geometrical or volumetric datasets. For instance, Elvins and Jain [10] proposed to use a density histogram to describe a volume dataset. Though simple, it provides very low discrimination power. Other different feature descriptors have been proposed to accomplish similarity assessment, including transformational [11], topological [15], and statistical [23] signatures. Different from these methods, our approach generates a unique 2D signature map of a 3D fiber model for further comparison and exploration.

2.2 DTI Fiber Model Exploration

Exploring and manipulating a DTI fiber model in the 3D space pose many challenges, especially on providing intuitive interaction. Embedding the fibers into a 2D space with projection techniques has been demonstrated to be an

effective means to study fiber models. Chen et al. [4] designed a novel interface by utilizing the multidimensional scaling (MDS) technique to facilitate quick and accurate 3D fiber selection on a 2D plane. Similarly, Jianu et al. [17] introduced a visual exploration paradigm by embedding 3D fibers on a 2D plane to reduce navigation efforts. Poco et al. [25] exploited the *Local Affine Multidimensional Projection (LAMP)* [19] technique to support fast visual exploration of large collection of DTI fibers. Demiralp et al. [9] presented a 2D path representations with a planar projection technique for studying fiber dataset. A web interface was also designed to support exploration. In general, the 2D visual representation captures the structures and patterns of the source dataset and is free of occlusion during interaction and exploration. However, most of these approaches focus on single fiber model exploration. This paper advances a computation-efficient two-phase projection technique to compare multiple fiber models.

3 Our Approach

Fig. 1 shows a schematic overview of our approach. In general, our approach consists of three main components. The preprocessing component registers all DTI volumes into a common space and reconstructs a 2nd order tensor in each voxel based on the Gaussian diffusion model. Fibers are then extracted according to the user-defined tracking parameters. Instead of direct comparing fiber models in the 3D space, we employ a two-phase projection technique followed by the density estimation to reformulate each fiber model as a 2D signature map. As a key benefit, these maps allow for intuitive recognition and quick comparison. A number of views and interactions are provided to discover and study differences among fiber models.

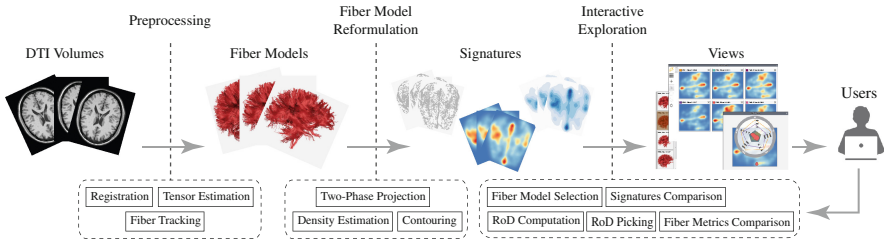

Fig. 1. An overview of our difference computation, visualization, and exploration pipeline for DTI fiber models.

3.1 Preprocessing

For accurate comparison, the alignment of all DTI volume datasets to a target is required. In our approach, FLIRT [16] is employed to perform a rigid registration.

After registration, a diffusion tensor field can be reconstructed of a DTI dataset. By tracing paths with numerical integration methods such as the second-order Runge-Kutta (RK2), a fiber model that captures the connectivity information of a DTI dataset is produced.

3.2 Fiber Model Reformulation

Let $\Gamma = F_1 \cup F_2 \cup ... \cup F_N$ be a fiber corpus consisting of N fiber models, and fiber model $F_i = \{f_i^j, j = 1, 2, ..., N_i\}$ has N_i fibers, where f_i^j denotes a fiber. To represent the variations among different fiber models, our approach generates a unique signature map S_i for each fiber model F_i.

Directly representing each fiber model F_i in the 3D space may cause visual clutter. Projection techniques [4,25] that focus on building a 2D visual representation for a fiber model can alleviate this issue. Before projection, all fibers must be reparameterized to make sure that they have the same number of vertices and orientations in order to calculate similarity measure used in LAMP technique [19,25].

To embed fibers on the visual plane, our approach employs the *Landmark MDS (LMDS)* technique [8] which performs a two-phase projection. A subset of fibers $\Gamma_{landmark} \subset \Gamma$ are selected from the fiber corpus as *landmark fibers*. Using these fibers as landmarks, LMDS can project each fibers $r \in \Gamma$ to its 2D location l_r on the visual plane. Throughout this paper, the longer mean of thresholded closest distance [30] is used to measure the dissimilarity between fibers:

$$d(p, q, t) = max(d_t(p, q, t), d_t(q, p, t)), \tag{1}$$

where $d_t(p, q, t) = mean_{u \in p, (min_{v \in q} \| u - v \| > t)} min_{v \in q} \parallel u - v \parallel$, u and v are vertices of fiber p and q respectively. The minimum threshold t is set to 0.5 mm as suggested by [30].

Compared with other methods, this projection scheme reduces the computational complexity of dissimilarity estimation from $O(n^2)$ to $O(m^2 + m \times n)$. $m = |\Gamma_{landmark}|$ is the number of landmark fibers. $n = |\Gamma|$ is the number of fibers in the fiber corpus. Empirically, m is set to $\sqrt{n}$ in our implementation. One additional benefit of this scheme is its intrinsic parallelizability, because each fiber is embedded independently from each other using a fixed linear transformation.

In our implementation, we randomly selected 100 landmark fibers as random selection produces similar results to those use optimized selection methods provided in [8].

Density Estimation. The embedding of each fiber model F_i yields a 2D scatterplot (see Fig. 5 second row). Similar fibers are positioned close to each other in this scatterplot. To facilitate recognition and visualization, we further apply the kernel density estimation (KDE) to the scatterplot to produce a continuous 2D density map D_i (see Fig. 5 third row). A Gaussian kernel is used in our approach with the bandwidth h determined by the Silverman's rule of thumb [27] and can be modified by the user.

By dividing the range of the computed density into multiple intervals and coloring the elements within each interval, another contour-like map (see Fig. 5 fourth row) is generated. The contoured density map suppresses many undesired details for a quick comparison.

Consequently, each fiber model uniquely determines a signature map S_i: a discrete scatterplot associated with a continuous density map and a contoured density map.

3.3 Region of Difference Estimation

The *Juxtaposition* design that displays visualizations side by side in multiple views is a common way to explore differences and similarities among multiple datasets. However, it requires a large amount of mental workload to identify the differences. Inspired by [26], we employ an explicit difference encoding to assist users in identifying regions of differences (RoDs).

Specifically, the density variance $V(x)$ at each location x is computed as:

$$V(x) = \frac{1}{N}\sum_{i=1}^{N}(D_i(x) - \mu(x))^2, \tag{2}$$

where $\mu(x)$ is the average density at location x. In our implementation, we compute the density variance for each pixel of the densities generated by KDE. Then, a user-adjustable threshold is used to filter out pixels of low density variations. At last, the region growing algorithm [26] is employed to group disjoint pixels into regions. The resultant RoDs provide an overview of differences residing in the shown signatures. Users can flexibly pick a RoD to further explore the statistical differences of fibers embedded into this region.

As RoDs are generated from the results of density estimation, they are affected by the bandwidth h of the kernel function. When bandwidth increased, number of RoDs will be reduced and adjacent RoDs tend to merge together.

4 Visual Exploration Interface

The fiber models, the generated signatures, and the computed RoDs can be interactively explored in our integrated interface composed of a set of linked views. Figure 2 illustrates an overview of this interface.

Fiber Model List View. Each fiber model is represented as a rectangular glyph. Basic information and a snapshot are embedded (see Fig. 2(a)). The fiber models of interest can be dragged to the signature view for further exploration and comparison.

Signature View. Users can compare the signatures in the signature view to discover differences and similarities among fiber models. The signature view employs a juxtapositional design which shows the selected fiber models' signatures in a side-by-side fashion. Users can remove a signature from this view. In addition, following interactions are supported:

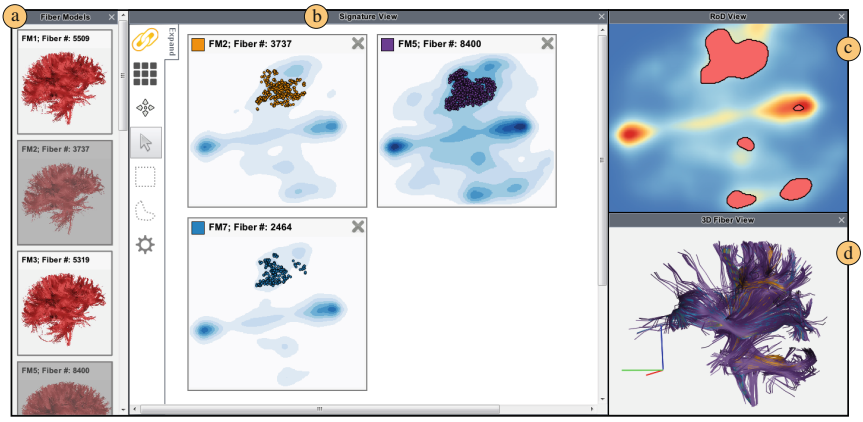

Fig. 2. The main views of our visual exploration interface. (a) The fiber model list view. (b) The signature view. (c) The RoD view. (d) The 3D fiber view.

Switching. Users can choose different forms of signatures (including the discrete scatterplot, the continuous density map, and the contoured density map) to be displayed.

Dragging. To facilitate comparison, signatures of interest can be dragged close to each other.

Selection. The *box* selection and *lasso* selection are provided to specify a region of interest. Linked selection simultaneously specify identical regions on different signatures. The selected fibers are shown in the 3D fiber view.

RoD View. As described above, the signature view shows the details of the selected fiber models' signatures. The identified RoDs are rendered as polygons overlaid on the average density map (see Fig. 2(c)). The Focus+Context interaction is implemented to inspect each individual RoD. Once users pick a RoD, a *DiffRadar* diagram will be displayed around. The *DiffRadar* diagram shows the detailed statistical variations of the selected fibers.

Figure 3 illustrates the design of our *DiffRadar* diagram. The radial layout is leveraged where each quantitative fiber metric corresponds to one of the equiangular axes. Five widely used fiber metrics are computed for those fibers embedded into the selected RoD: number of fibers (NF), total length (TL), average total length (ATL), total FA weighted length (TWL), and average FA weighted length (ATWL). Please refer to [5] for the computation details. The picked RoD is shown in the center of this diagram. The metrics of a fiber model are connected with polylines. To differentiate fiber models, a categorical color set is used.

3D Fiber View. As the axes in signatures do not have intrinsic meanings, linked views and interactions are demanded. Fibers selected from either the signature view or the RoD view are visualized as illuminated lines [21] in the 3D space. Users can easily understand and verify the findings in this view.

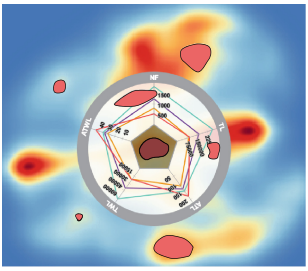

Fig. 3. An example *DiffRadar* diagram. The average density map is displayed at background as a context. RoDs are shown as polygons.

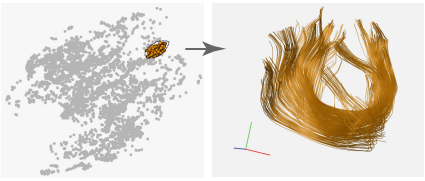

Fig. 4. Linked exploration: selected fibers in the signature view (a) are immediately rendered as illuminated lines in the 3D fiber view (b).

5 Results and Discussions

We implemented our approach based on a set of toolkits and libraries. The preprocessing is accomplished using a free software library FSL. Typically several minutes are needed to pre-compute a fiber model on our experimental platform. The algorithms (Sect. 3.2) are implemented with the standard C++. Computing dissimilarities between fibers are further accelerated with CUDA 5.5. The visualization interface is developed based on Qt 5.1. The rendering of DTI fibers utilized a GPU-accelerated illuminated line algorithm [21].

5.1 Fiber Model Characterization

We tested our approach on a set of 78 DTI data. Some of the subjects were scanned multiple times in the data.

The signatures generated with our approach characterize the overall structures and distributional patterns of each fiber model. The scatterplot reveals the similarities among fibers. Similar fibers are positioned close to each other. It is thus natural to perform feature exploration by studying the shape, layout, and distribution in this map. Users can select a region of interest and inspect the selected fibers in the 3D space (see Fig. 4).

Figure 5 shows the signatures of three healthy subjects **FM1**, **FM2**, and **FM3**. Generally, all of them present similar low-dimensional patterns. We can further inspect the detailed differences among them in the RoD view as shown in Fig. 6. From the *DiffRadar* diagram for RoD **R1** in Fig. 6(a), we find that subject **FM1** has much lower values in terms of quantitative metrics NF, TL, and TWL. However, as shown in Fig. 6(b) for RoD **R2**, subject **FM1** has slightly higher values in terms of these quantitative metrics compared to subject **FM2** and **FM3**. Anatomical variations mainly contribute to these differences.

5.2 DTI Tracking Parameter Study

This experiment intends to investigate whether the integration step size has a great influence on the tracking results. For this purpose, we generate several

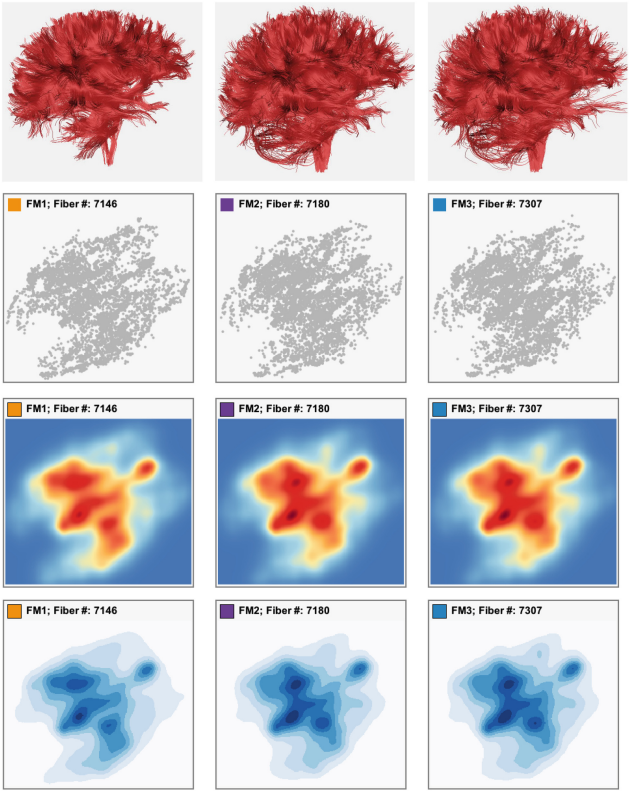

Fig. 5. Results for three fiber models selected from the atlas dataset. From top to bottom: the 3D fiber models, the 2D embedding, the continuous density maps, and the contoured density maps.

fiber models from a single DWI image with varied integration step size. Some of them have same integration step but few differences are caused by jittering of seeding locations. We selected six signatures which corresponding integration steps are 0.75, 0.75, 0.58, 0.58, 0.58 and 0.58.

The computed RoDs in Fig. 7(a) explicitly show the major differences among them. This indicate that the integration step size has a strong effect on the tracking results. That is because the step size determines how long a fiber can move forward and backward in the path tracing process. We also compute the RoDs for the last four signatures (see Fig. 7(b)). It can be easily verified that fewer RoDs are identified compared with Fig. 7(a), because there are smaller variations among the last four signatures.

5.3 Discussions and Future Work

Our approach shows promising effectiveness in displaying differences among fiber models. It can be regarded as an adaption of the low-dimensional projection

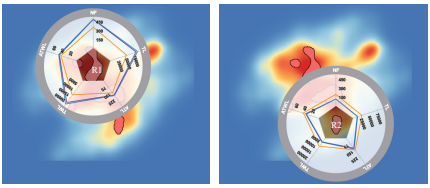

Fig. 6. The *DiffRadar* diagrams for two RoDs: **R1** and **R2**. The variation of **R1** is higher than that of **R2**.

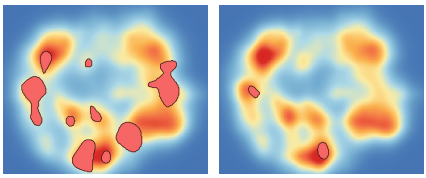

Fig. 7. (a) The RoDs for six signatures. (b) The RoDs for the last four signatures. The same threshold is used.

scheme proposed in [4,17,25] to multiple datasets comparisons. Our projection scheme uses the same set of *landmark fibers* to build low-dimensional representations for fiber models. The low-dimensional embedding of the *landmark fibers* can be regarded as the backbone of these low-dimensional representations.

The axes of the low-dimensional projection layout do not have physical meanings. Understanding the projection depends on the user's ability to link locations in the 2D plane to the fibers in the 3D space. Our approach exploits the linked interaction to provide a fast and intuitive correspondence between points in the 2D embedding space and 3D fibers. However, it requires training and exploration time. We plan to enhance the correspondence between the 2D embedding space and the 3D space. One possibility is to label some representative fibers in the 2D embedding space.

Due to the limited human perception capability and screen space, it is challenging to simultaneously compare a large number of signatures in the signature view. The RoD view shows an overview to locate differences among them. However, when diving into the details, visual clutter might be produced in the *DiffRadar* diagram caused by too many overlapped polylines. Clustering and hierarchical exploration are a feasible solution as proven by [26]. This is an avenue for our future work. In addition, effective comparison models will be further studied as well.

6 Conclusion

This paper presents a novel comparative visualization approach for discovering and exploring differences among DTI fiber models. While previous methods compare DTI datasets in either a 3D physical space or a statistical metric space, our approach compares the datasets in a common embedding space. The core is a computation-efficient two-phase projection technique followed by a density estimation process to build the low-dimensional representations of fiber models. Using these low-dimensional representations, regions of significant differences are further explicitly computed. An integrated interface is designed to explore the differences. Experiments on different DTI datasets demonstrate the effectiveness of this approach. Some experts gave positive comments that being able to quickly compare and explore different fibers models with each other is definitely useful.

Acknowledgment. This work is supported by NSFC (61232012, 61422211, 61303141), Zhejiang NSFC (Y12F020172), and the Fundamental Research Funds for the Central Universities.

References

1. Basser, P.J., Pajevic, S., Pierpaoli, C., Duda, J., Aldroubi, A.: In vivo fiber tractography using DT-MRI data. Magn. Resonance Med. **44**, 625–632 (2000)
2. Basser, P.J., Pierpaoli, C.: A simplified method to measure the diffusion tensor from seven MR images. Magn. Resonance Med. **39**, 928–934 (1998)
3. Brecheisen, R., Vilanova, A., Platel, B., ter Haar Romeny, B.: Parameter sensitivity visualization for DTI fiber tracking. IEEE Trans. Vis. Comput. Graph. **15**(6), 1441–1448 (2009)
4. Chen, W., Ding, Z., Zhang, S., MacKay-Brandt, A., Correia, S., Qu, H., Crow, J.A., Tate, D.F., Yan, Z., Peng, Q.: A novel interface for interactive exploration of DTI fibers. IEEE Trans. Vis. Comput. Graph. **15**(6), 1433–1440 (2009)
5. Corouge, I., Fletcher, P.T., Joshi, S., Gouttard, S., Gerig, G.: Fiber tract-oriented statistics for quantitative diffusion tensor MRI analysis. Med. Image Anal. **10**(5), 786–798 (2006)
6. Correia, S., Lee, S.Y., Voorn, T., Tate, D.F., Paul, R.H., Zhang, S., Salloway, S.P., Malloy, P.F., Laidlaw, D.H.: Quantitative tractography metrics of white matter integrity in diffusion-tensor MRI. Neuroimage **42**(2), 568–581 (2008)
7. DaSilva, M.J., Zhang, S., Demiralp, C., Laidlaw, D.H.: Visualizing the differences between diffusion tensor volume images. In: Proceedings of the International Society for Magnetic Resonance in Medicine Diffusion MRI Workshop (2000)
8. De Silva, V., Tenenbaum, J.B.: Sparse multidimensional scaling using landmark points. Technical report, Stanford University (2004)
9. Demiralp, C., Jianu, R., Laidlaw, D.H.: Exploring brain connectivity with two-dimensional maps. In: Laidlaw, D.H., Vilanova, A. (eds.) New Developments in the Visualization and Processing of Tensor Fields. Mathematics and Visualization, pp. 187–207. Springer, Heidelberg (2012)
10. Elvins, T.T., Jain, R.: Web-based volumetric data retrieval. In: Proceedings of the First Symposium on Virtual Reality Modeling Language, pp. 7–12. ACM (1995)
11. Funkhouser, T., Min, P., Kazhdan, M., Chen, J., Halderman, A., Dobkin, D., Jacobs, D.: A search engine for 3D models. ACM Trans. Graph. **22**(1), 83–105 (2003)
12. Gleicher, M., Albers, D., Walker, R., Jusufi, I., Hansen, C.D., Roberts, J.C.: Visual comparison for information visualization. Inf. Vis. **10**(4), 289–309 (2011)
13. Goodlett, C.B., Fletcher, P.T., Gilmore, J.H., Gerig, G.: Group statistics of DTI fiber bundles using spatial functions of tensor measures. In: Metaxas, D., Axel, L., Fichtinger, G., Székely, G. (eds.) MICCAI 2008, Part I. LNCS, vol. 5241, pp. 1068–1075. Springer, Heidelberg (2008)
14. Hagmann, P., Jonasson, L., Maeder, P., Thiran, J.P., Wedeen, V.J., Meuli, R.: Understanding diffusion MR imaging techniques: from scalar diffusion-weighted imaging to diffusion tensor imaging and beyond 1. Radiographics **26**(suppl 1), S205–S223 (2006)
15. Hilaga, M., Shinagawa, Y., Kohmura, T., Kunii, T.L.: Topology matching for fully automatic similarity estimation of 3D shapes. In: Proceedings of the 28th Annual Conference on Computer Graphics and Interactive Techniques, pp. 203–212. ACM (2001)

16. Jenkinson, M., Bannister, P., Brady, M., Smith, S.: Improved optimization for the robust and accurate linear registration and motion correction of brain images. Neuroimage **17**(2), 825–841 (2002)
17. Jianu, R., Demiralp, C., Laidlaw, D.H.: Exploring 3d DTI fiber tracts with linked 2d representations. IEEE Trans. Vis. Comput. Graph. **15**(6), 1449–1456 (2009)
18. Jiao, F., Phillips, J.M., Gur, Y., Johnson, C.R.: Uncertainty visualization in hardi based on ensembles of ODFs. In: IEEE Pacific Visualization Symposium (PacificVis), pp. 193–200. IEEE (2012)
19. Joia, P., Paulovich, F.V., Coimbra, D., Cuminato, J.A., Nonato, L.G.: Local affine multidimensional projection. IEEE Trans. Vis. Comput. Graph. **17**(12), 2563–2571 (2011)
20. Malik, M.M., Heinzl, C., Groeller, M.E.: Comparative visualization for parameter studies of dataset series. IEEE Trans. Vis. Comput. Graph. **16**(5), 829–840 (2010)
21. Mallo, O., Peikert, R., Sigg, C., Sadlo, F.: Illuminated lines revisited. In: Proceedings of IEEE Visualization, pp. 19–26. IEEE (2005)
22. Oelke, D., Strobelt, H., Rohrdantz, C., Gurevych, I., Deussen, O.: Comparative exploration of document collections: a visual analytics approach. Comput. Graph. Forum **33**, 201–210 (2014). Wiley Online Library
23. Osada, R., Funkhouser, T., Chazelle, B.: Shape distributions. ACM Trans. Graph. **21**(4), 93–101 (2002)
24. Pajevic, S., Basser, P.J.: Parametric and non-parametric statistical analysis of DT-MRI data. J. Magn. Resonance **163**(1), 1–14 (2003)
25. Poco, J., Eler, D.M., Paulovich, F.V., Minghim, R.: Employing 2d projections for fast visual exploration of large fiber tracking data. Comput. Graph. Forum **31**, 1075–1084 (2012). Wiley Online Library
26. Schmidt, J., Groller, M.E., Bruckner, S.: Vaico: visual analysis for image comparison. IEEE Trans. Vis. Comput. Graph. **19**(12), 2090–2099 (2013)
27. Silverman, B.: Density estimation for statistics and data analysis. Chapman & Hall/CRC, Boca Raton (1986)
28. Smith, S.M., Jenkinson, M., Johansen-Berg, H., Rueckert, D., Nichols, T.E., Mackay, C.E., Watkins, K.E., Ciccarelli, O., Cader, M.Z., Matthews, P.M., et al.: Tract-based spatial statistics: voxelwise analysis of multi-subject diffusion data. Neuroimage **31**(4), 1487–1505 (2006)
29. Verma, V., Pang, A.: Comparative flow visualization. IEEE Trans. Vis. Comput. Graph. **10**(6), 609–624 (2004)
30. Zhang, S., Correia, S., Laidlaw, D.H.: Identifying white-matter fiber bundles in DTI data using an automated proximity-based fiber-clustering method. IEEE Trans. Vis. Comput. Graph. **14**(5), 1044–1053 (2008)